Original Article

Hsa_circ_0079530/AQP4 Axis Is Related to Non-Small Cell Lung Cancer Development and Radiosensitivity

Xianghui Yang,[1] Min Li,[2] Yang Zhao,[1] Xiaolang Tan,[1] Jiqing Su,[1] and Xi Zhong[3]

Background: Circular RNAs are associated with non-small cell lung cancer (NSCLC) development and radiosensitivity. Nevertheless, the function and regulation mechanism of hsa_circ_0079530 (circ_0079530) in NSCLC development and radiosensitivity are largely unknown.
Methods: The abundances of circ_0079530, microRNA (miR-409-3p), aquaporin 4 (AQP4), E-cadherin, intercellular adhesion molecule-1, vitronectin, proliferating cell nuclear antigen, and matrix metalloproteinase 9 were determined via quantitative reverse transcription polymerase chain reaction or western blotting. Cell proliferation, survival fraction, cycle process, migration, invasion, and *in vivo* growth were examined by cell counting kit-8, colony formation, flow cytometry, transwell, and xenograft analyses. The binding relationship was assessed via dual-luciferase reporter assay and RNA immunoprecipitation assay.
Results: Circ_0079530 expression was increased in NSCLC tissues and radioresistant samples. Circ_0079530 knockdown restrained cell proliferation, migration, and invasion, and facilitated radiosensitivity. Circ_0079530 silence decreased tumor growth with or without radiation treatment. Circ_0079530 was verified as a miR-409-3p sponge, and miR-409-3p downregulation mitigated the effects of circ_0079530 interference on NSCLC cell malignancy and radiosensitivity. AQP4 was directly targeted by miR-409-3p. MiR-409-3p restrained cell proliferation, migration, and invasion, and enhanced radiosensitivity by decreasing AQP4 expression. Notably, circ_0079530 silence decreased AQP4 expression by regulating miR-409-3p expression.
Conclusion: Circ_0079530 silence repressed cell proliferation, migration, and invasion, and facilitated radiosensitivity in NSCLC cells by mediating miR-409-3p/AQP4 axis.

Keywords: AQP4, circ_0079530, radiosensitivity, miR-409-3p, non-small cell lung cancer

---

[1]*Department of Oncology, Changsha Central Hospital, Changsha, China*
[2]*Interventional Therapy Centre, Changsha Central Hospital, Changsha, China*
[3]*Department of Oncology, People's Hospital of Ningxiang, Ningxiang, Changsha, China*

Corresponding author: Xi Zhong. Department of Oncology, People's Hospital of Ningxiang, No. 209, North Yihuan Road, Yutan Street, Ningxiang, Hunan 410600, China
Email: zhongxi5200@163.com

Introduction

Lung cancer is a frequent cancer with high cancer-associated deaths.[1] Non-small cell lung cancer (NSCLC) represents approximately 85% of lung cancer, and mainly includes adenocarcinoma (40%), squamous cell carcinoma (30%), and large cell carcinoma (15%).[2] The diagnosis and treatment of NSCLC have gained significant progress, while the 5-year survival rate remains lower than 68%.[3] Radiotherapy is a common treatment approach of advanced NSCLC.[4] However, the loss of radiosensitivity limits the effect of radiotherapy. Hence, exploring new targets are highly desirable for regulation of NSCLC progression and radiosensitivity.

Circular RNAs (circRNAs) are a class of closed noncoding RNAs that are generated by back-splicing events from linear primary transcripts.[5] According to reports, circRNAs are important regulators of tumorigenesis, including NSCLC.[6] For instance, circRNA protein tyrosine phosphatase receptor type A (circRNA_PTPRA) repressed cell malignancy in NSCLC,[7] circRNA carboxypeptidase A4 (CPA4) (hsa_circ_0082374) promoted NSCLC cell malignant behaviors.[8] Moreover, circRNAs can function as microRNA (miRNA) sponges to regulate the downstream mRNAs via miRNA response elements, thus mediating NSCLC progression.[9] For example, circRNA metadherin.4 (MTDH.4) acts as a sponge of miR-630 and regulates astrocyte elevated gene-1 expression by adsorbing miR-630, thus promoting cell proliferation, migration, invasion, and chemo- and radioresistance in NSCLC.[10] The hsa_circ_0079530 (circ_0079530) is a circRNA derived from the Twist1 gene, which predicts the worse outcomes of NSCLC patients and promotes cell proliferation and invasion.[11] However, the function of circ_0079530 in radiosensitivity and its regulation mechanism in NSCLC progression remain uncertain.

MiRNAs can target gene expression involved in NSCLC progression via targeting the 3' untranslated region (UTR) of downstream mRNAs.[12] For example, miR-21 promotes NSCLC growth, metastasis, and chemo- and radioresistance via regulating phosphatase and tensin homolog expression,[13] while miR-300 curbs NSCLC cell invasion and migration via downregulating ETS proto-oncogene 1 (ETS1).[14] Three miRNAs (miR-409-3p, miR-543, and miR-576-5p) that might interact with circ_0079530 were jointly predicted by the two tools. MiR-409-3p suppresses NSCLC growth and metastasis.[15,16] Nevertheless, the function of miR-409-3p in radiosensitivity is uncertain, and whether it is associated with circ_0079530-mediated function in NSCLC is unclear.

Aquaporins (AQPs) play important roles in respiratory diseases, including NSCLC.[17] Aquaporin 4 (AQP4) is a key member of AQPs that is associated with NSCLC invasion.[18] Moreover, AQP4 is related to radiosensitivity in breast cancer,[19] but its role in radiosensitivity in NSCLC is unknown. Bioinformatics analysis predicted that miR-409-3p might target AQP4. Hence, we hypothesized that circ_0079530 might regulate the miR-409-3p/AQP4 axis to modulate NSCLC progression and radiosensitivity.

In this research, we uncovered a novel mechanism by which circ_0079530 promoted NSCLC progression and radioresistance by regulating the miR-409-3p/AQP4 axis.

Materials and Methods

Patients and samples

Sixty-seven NSCLC patients at stage II or III who underwent curative resection and postoperative radiotherapy (accumulated radiation dose of 60 Gy and weekly dose of 10 Gy) were enrolled in Changsha Central Hospital from April 2016 to March 2019. The radiation dose was 60 Gy over 6 to 7 weeks, as a 2 Gy/fraction with 5 fractions per week. The radiation response was assessed after the last-time radiotherapy for 3 weeks. According to the radiation response based on the Response Evaluation Criteria in Solid Tumors (RECIST) rules,[20] the patients were divided into radiosensitive (n = 36; including complete or partial response) or radioresistant (n = 31; including stable or progressive disease) group. The tumor tissues (n = 67) were collected, and adjacent non-tumor tissue (ANT) samples were used as controls. All tissues were maintained in liquid nitrogen. Each patient provided the written informed consent. This research was authorized by the ethics committee of Changsha Central Hospital.

Cell culture

Lung squamous cell carcinoma cell line (H2170 cells) (product number: CL-0394), lung adenocarcinoma cell line (A549 cells) (product number: CL-0016), and human embryonic lung cell line (MRC-5 cells) (product number: CL-0161) were obtained from Procell (Wuhan, China) and orderly maintained in Roswell Park Memorial Institute (RPMI)-1640 medium (Gibco, Grand Island, NY, USA), Ham's F-12K (Thermo Fisher Scientific, Waltham, MA, USA), or Minimum Essential Medium (MEM) (Thermo Fisher Scientific) plus 10%

fetal bovine serum (FBS) (Gibco) and 1% penicillin/streptomycin (Gibco) at 37°C and 5% CO_2. The cell culture medium was replaced when cells were cultured for 3–4 days.

Cell transfection

AQP4 overexpression vector was constructed using the empty pcDNA3.1 vector (Thermo Fisher Scientific). Small interfering RNA (siRNA) for circ_0079530 (si-circ_0079530-1, si-circ_0079530-2, and si-circ_0079530-3), miR-409-3p mimic, miR-409-3p inhibitor (anti-miR-409-3p), and their negative controls (si-NC, miR-NC, and anti-NC) were generated from Genomeditech (Shanghai, China). All oligonucleotide sequences are displayed in **Supplementary Table 1** (all supplementary files are available online.). Then, H2170 and A549 cells were incubated with constructed vectors or oligonucleotides and Lipofectamine 2000 (Thermo Fisher Scientific) for 24 h.

Quantitative reverse transcription-polymerase chain reaction (qRT-PCR)

Total RNA was extracted through TRIzol (Thermo Fisher Scientific). The miRNA or M-MLV Reverse Transcriptase kit (Thermo Fisher Scientific) was used to generate cDNA with 800 ng RNA, followed by a mixture with SYBR (TaKaRa, Otsu, Japan) and primer pairs for qRT-PCR analysis. The primer pairs were exhibited in **Supplementary Table 2**. Glyceraldehyde-3-phosphate dehydrogenase (GAPDH) or U6 functioned as a control. Relative RNA expression was determined via the $2^{-\Delta\Delta C_t}$ method.

RNase R and Actinomycin D assays

RNase R and Actinomycin D assays were performed to analyze the circular structure of circRNA. In brief, total RNA was incubated by 2 U/μg RNase R (Geneseed, Guangzhou, China) for 15 min and subjected to qRT-PCR for analysis of circ_0079530 and GAPDH. For Actinomycin D analysis, H2170 and A549 cells were subjected to 2 μg/mL Actinomycin D (Sigma, St. Louis, MO, USA) for different times and then qRT-PCR was applied to analyze the abundances of circ_0079530 and GAPDH.

Cell counting kit-8 (CCK-8)

For cell proliferation analysis, 1×10^4 A549 and H2170 were seeded in 96-well plates, followed by addition with 10 μL CCK-8 (Beyotime, Shanghai, China) after 24, 48, or 72 h. The OD value at 450 nm was determined through a microplate reader.

Radiation treatment and colony formation assay

Colony formation assay was used to investigate radiosensitivity. H2170 and A549 cells in 25-T flasks were irradiated by different doses (0, 1, 2, 4, or 8 Gy) of radiation with an X-ray linear accelerator (Elekta, Beijing, China) at a dose rate of 1 Gy/min. Then, 800 cells/well were seeded in 6-well plates. After 12 days, colonies were dyed to 0.1% crystal violet (Solarbio, Beijing, China) and imaged.

EdU assay

Briefly, 5×10^4 H2170 and A549 cells with or without radiation treatment were added in 6-well plates and cultured for 24 h. Next, cells were treated with 50 μM of EdU (RiboBio, Guangzhou, China) at 37°C, followed by incubation for 2 h. After fixation in 4% formaldehyde for 30 min, treated cells were added with 0.5% Triton X-100, followed by reaction with Apollo. Also, 4',6-diamidino-2-phenylindole (DAPI) was applied to identify the nuclei. In the end, a microscope (Olympus, Tokyo, Japan) was used to analyze the proliferation-positive cells.

Transwell analysis

Cell invasion was analyzed using Matrigel-coated transwell chamber (Corning Inc., Corning, NY, USA), and migration was detected using transwell chamber, which did not have Matrigel. In brief, H2170 and A549 cells with or without radiation treatment H2170 and A549 cells (5×10^5 cells for invasion analysis and 1×10^5 cells for migration analysis) in free-serum RPMI-1640 medium were added in the upper chambers. Lower chambers were added with 600 μL RPMI-1640 medium plus 10% FBS. After 24 h, 0.1% crystal violet was used to stain the cells in the lower counterpart, followed by analysis using a microscope (Olympus, 100× magnification). Migratory or invasive number was determined with ImageJ v1.6 (NIH, Bethesda, MD, USA).

Western blotting

The radioimmunoprecipitation assay buffer (Thermo Fisher Scientific) was used to isolate the total protein. Following quantification with bicinchoninic acid kit (Thermo Fisher Scientific), 20 μg samples were separated via sodium dodecyl sulfate–polyacrylamide gel electrophoresis and transferred on the polyvinylidene fluoride membrane (Bio-Rad, Hercules, CA, USA). The membranes were blocked in 5% fat-free milk for 1 h and then incubated with primary antibodies (E-cadherin [ab40772, 1:8000; Abcam, Cambridge, UK], intercellular

adhesion molecule-1 [ICAM-1] [ab109361, 1:1000; Abcam], vitronectin [ab45139, 1:2000; Abcam], proliferating cell nuclear antigen [PCNA] [ab18197, 1:5000; Abcam], matrix metalloproteinase 9 [MMP9] [ab76003, 1:5000; Abcam], AQP4 [ab81355, 1:300; Abcam], and GAPDH [1:5000; Abcam]) overnight, followed by interacting with secondary antibodies (ab6721, 1:2000; Abcam) for 2 h. Then blots were exposed to enhanced chemiluminescence (Solarbio) and detected via ImageJ v1.8, with GAPDH as a normalized control.

Xenograft model

The lentivirus-carrying short hairpin RNA targeting circ_0079530 (sh-circ_0079530) or negative control (sh-NC) was constructed by Genomeditech and followed by infection of H2170 cells according to the instructions. Six-week-old male BALB/c nude mice (Vital River, Beijing, China) were divided into four groups (n = 6; sh-NC, sh-circ_0079530, sh-NC + 4 Gy, and sh-circ_0079530 + 4 Gy), followed by subcutaneous injection with 2×10^6 H2170 cells with sh-circ_0079530 or sh-NC. After five days of growth, a group of mice with sh-NC and sh-circ_0079530 was exposed to 4 Gy radiation at the tumor site, respectively. Tumor volume was examined every 5 days with a formula $(0.5 \times \text{length} \times \text{width}^2)$. The body weight of mice had no significant difference, and no unexpected deaths occurred in each group. A month later, mice were euthanized with inhalation anesthesia of 5% isoflurane (Sigma). Tumors were harvested, weighed, and followed via collection for protein detection. Animal experiments were permitted by the Animal Ethics Committee of Changsha Central Hospital.

Dual-luciferase reporter assay

The miRNAs that might interact with circ_0079530 were predicted by circInteractome (https://circinteractome.nia.nih.gov/) and starBase (http://starbase.sysu.edu.cn/), and the targets of miR-409-3p were predicted by starBase. The wild-type (WT) sequence of circ_0079530 or AQP4 3'UTR with miR-409-3p binding sites was introduced in the pmir-GLO vector (Promega, Madison, WI, USA), acquiring the WT-circ_0079530 and WT-3'UTR AQP4 vectors. Also, mutant (MUT)-circ_0079530 and MUT-3'UTR AQP4 vectors were constructed using the sequence containing the MUT binding sites of miR-409-3p. The constructed vectors were co-transfected with miR-409-3p mimic or miR-NC into H2170 and A549 cells, followed by analysis using a dual-luciferase reporter assay kit (Promega) according to the instructions.

RNA immunoprecipitation (RIP)

In short, H2170 and A549 cells at 80% confluency were harvested, followed by introduction with complete RIP lysis buffer (Millipore, Billerica, MA, USA). Then, the cell extracts were incubated with RIP buffer with magnetic beads conjugated with anti-Argonaute2 (Ago2) antibody or negative control immunoglobulin G (IgG). After digesting with proteinase K, the samples were analyzed using qRT-PCR assay.

Immunohistochemistry (IHC)

In this assay, the samples of radiosensitive, radioresistant, and ANT tissues were first fixed in 4% paraformaldehyde, dehydrated, and embedded in paraffin. Whereafter, 5-μm-thick sections were cut, followed by staining with hematoxylin and eosin for histopathology using a microscope (Olympus). For detecting the level of AQP4, the sections were washed with PBS and incubated with a primary antibody AQP4 (ab128906, 1:200 dilution; Abcam) at 4°C overnight. Finally, images were acquired for analysis.

Statistical analysis

Data were shown as mean ± standard deviation (SD) from 3 experiments. The Pearson coefficient test analyzed the linear relationship of RNA level in NSCLC tissues. The Student's t-test or one-way analysis of variance with the Tukey's post hoc test was used for comparison of the group difference, which was processed using GraphPad Prism 8 (GraphPad Inc., La Jolla, CA, USA). $P <0.05$ predicted the significant difference.

Results

Circ_0079530 expression is increased in NSCLC

To analyze if circ_0079530 was associated with NSCLC development and radiosensitivity, circ_0079530 expression was detected in cancer tissues. Circ_0079530 abundance was markedly enhanced in NSCLC tumor tissue samples (n = 67) compared with ANT samples (n = 67), and circ_0079530 expression was higher in radioresistant samples (n = 36) than in radiosensitive tissues (n = 31) (**Supplementary Fig. 1A**). In the 67 patients, 61 cases displayed high expression of circ_0079530 in cancer tissues, while circ_0079530 abundance was lower in cancer tissues of 6 cases than normal samples (**Supplementary Fig. 1B**). Moreover, circ_0079530 level was clearly upregulated in H2170 and A549 cells in comparison to the MRC-5 cells (**Supplementary Fig. 1C**). Additionally, the stability and circular structure of circ_0079530 were analyzed via RNase

R and Actinomycin D assays. The results showed that RNase R and Actinomycin D exposure significantly decreased GAPDH abundance, but circ_0079530 was more resistant to RNase R and Actinomycin D than linear GAPDH (**Supplementary Figs. 1D** and **1E**). These results suggested that circ_0079530 was a typical circRNA that might be related to NSCLC radiosensitivity.

Circ_0079530 downregulation inhibits cell proliferation, migration, and invasion, but increases radiosensitivity in NSCLC cells

To study the role of circ_0079530 in NSCLC, circ_0079530 was decreased in H2170 and A549 cells. Three siRNAs for circ_0079530 effectively decreased circ_0079530 abundance, and si-circ_0079530-3 had the highest knockdown efficacy (**Fig. 1A**). Thus, cells transfected with si-circ_0079530-3 or si-NC were used for further studies. Circ_0079530 knockdown significantly decreased proliferation of H2170 and A549 cells (**Fig. 1B**). Furthermore, circ_0079530 interference exacerbated the reduction of survival fraction after radiation treatment, suggesting circ_0079530 enhanced the radiosensitivity of H2170 and A549 cells (**Fig. 1C**). In addition, cell cycle distribution was analyzed in cells with or without radiation treatment. As displayed in **Fig. 1D**, circ_0079530 knockdown clearly decreased EdU positive cells in the presence or absence of radiation, and the proliferation of circ_0079530-silenced NSCLC cells was overtly repressed under radiation treatment than that in the control group. We then further studied if circ_0079530 was involved in NSCLC metastasis. As shown in **Figs. 1E** and **1F**, circ_0079530 knockdown evidently constrained the migratory and invasive abilities of H2170 and A549 cells under radiation and non-radiation treatment, and radiation treatment further repressed the migration and invasion of circ_0079530-knockdown H2170 and A549 cells. Furthermore, circ_0079530 silence markedly increased E-cadherin protein levels and decreased ICAM-1 and vitronectin protein levels in H2170 and A549 cells with or without 4 Gy radiation treatment (**Fig. 1G**). In addition, radiation treatment resulted in an elevation in E-cadherin protein levels and a decrease in ICAM-1 and vitronectin protein levels in circ_0079530-inhibiting H2170 and A549 cells (**Fig. 1G**). These results showed that circ_0079530 silence repressed NSCLC cell migration and invasion under radiation and non-radiation conditions.

Circ_0079530 silence decreases tumor growth

To probe into the function of circ_0079530 *in vivo*, H2170 cells were used for the establishment of xenograft models. The H2170 cells with sh-circ_0079530 were constructed, and lentivirus-mediated sh-circ_0079530 effectively reduced circ_0079530 expression in H2170 cells compared with that in the sh-NC group (**Fig. 2A**). Circ_0079530 knockdown evidently reduced tumor volume and weight with or without radiation treatment, but the volume and weight of xenograft tumors were smaller and lower in the sh-circ_0079530 group under radiation treatment compared with those without radiation treatment (**Figs. 2B** and **2C**). Additionally, circ_0079530 downregulation obviously inhibited PCNA, MMP9, ICAM-1, and vitronectin protein levels with or without radiation treatment, while enhanced E-cadherin protein levels in the sh-circ_0079530 group (**Fig. 2D**). In addition, the protein levels of PCNA, MMP9, and ICAM-1 were lower in tumor tissues derived from the sh-circ_0079530 group under radiation treatment than tumor tissues derived from the sh-circ_0079530 group, but the levels of E-cadherin protein were higher (**Fig. 2D**). These data suggested that circ_0079530 knockdown inhibited NSCLC cell growth under radiation and non-radiation conditions.

Circ_0079530 is a sponge of miR-409-3p

To probe the mechanism modulated by circ_0079530, the miRNAs that might interact with circ_0079530 were analyzed by starBase and circInteractome. Three miRNAs were jointly predicted by the two tools, and miR-409-3p abundance was affected most by circ_0079530 silence compared with the other candidates (miR-543 and miR-576-5p) (**Fig. 3A**). Hence, miR-409-3p was chosen for subsequent experiments. The binding sequence of circ_0079530 and miR-409-3p is displayed in **Fig. 3B**. To confirm this prediction, WT-circ_0079530 and MUT-circ_0079530 luciferase reporter vectors were constructed. The overexpression or knockdown efficacy of miR-409-3p mimic or inhibitor (anti-miR-409-3p) is validated in **Fig. 3C**. Moreover, the luciferase activity of WT-circ_0079530 was clearly decreased via miR-409-3p mimic, but luciferase activity of MUT-circ_0079530 had no significant difference (**Fig. 3D**). Then, to further confirm the mutual effect of circ_0079530 and miR-409-3p, RIP assay was performed in H2170 and A549 cells. Data suggested that circ_0079530 and miR-409-3p were specifically enriched in Ago2 pellets in H2170 and A549 cells when compared with that in the IgG control group (**Figs. 3E** and **3F**). Additionally, miR-409-3p expression was evidently reduced in radiosensitive (n = 36) and
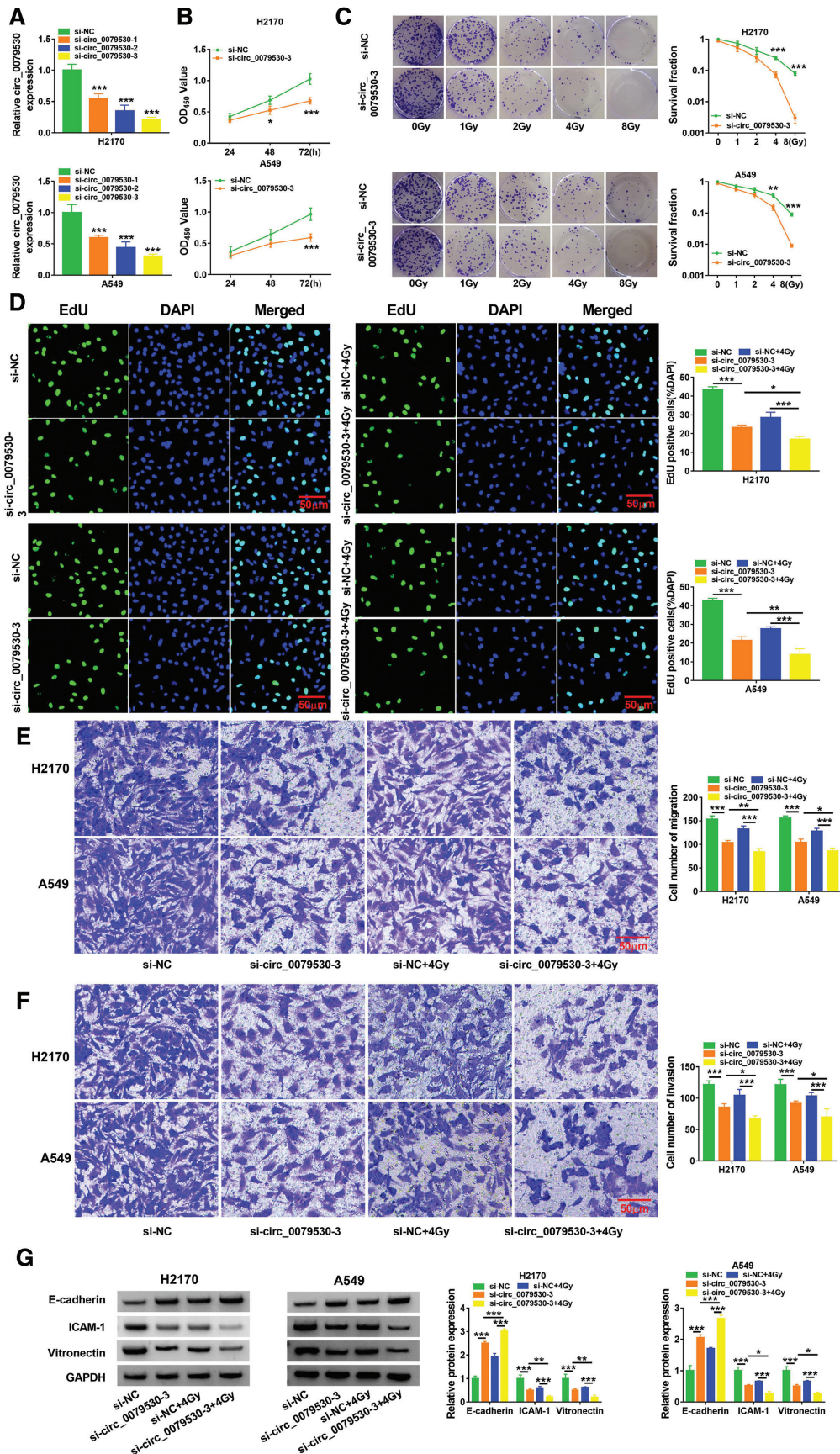
Fig. 1 (Continued)

Fig. 1 Circ_0079530 knockdown inhibits cell proliferation, migration, and invasion but enhances radiosensitivity in NSCLC. (**A**) Circ_0079530 level was measured via qRT-PCR in cells transfected with si-circ_0079530-1, si-circ_0079530-2, si-circ_0079530-3, or si-NC (n = 3). (**B**) Cell proliferation was measured via CCK-8 in si-circ_0079530-3 or si-NC-transfected cells (n = 3). (**C**) Radiosensitivity was analyzed by colony formation assay in si-circ_0079530-3 or si-NC-transfected cells after treatment of various doses of radiation (n = 3). (**D**) EdU-positive cells were assessed by EdU assay in cells transfected with si-circ_0079530-3 or si-NC after treatment with 4 Gy radiation or not (n = 3). (**E** and **F**) Cell migration and invasion were examined via transwell assay (n = 3). (**G**) E-cadherin, ICAM-1, and vitronectin levels were detected via western blotting in cells (n = 3). *P <0.05, **P <0.01, and ***P <0.001. NSCLC: non-small cell lung cancer; qRT-PCR: quantitative reverse transcription-polymerase chain reaction; NC: negative control; CCK-8: cell counting kit-8; ICAM-1: intercellular adhesion molecule-1
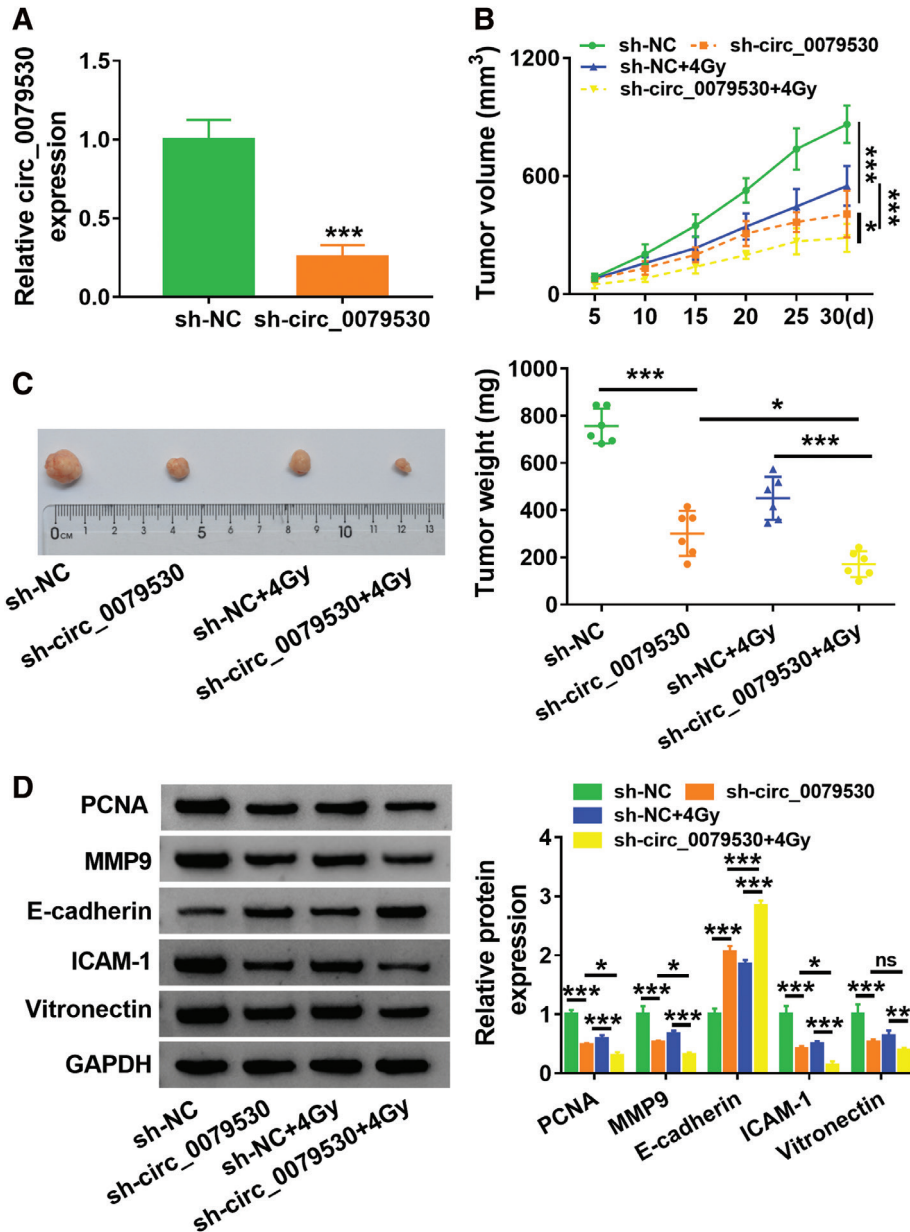
Fig. 2 Circ_0079530 knockdown suppresses tumor growth in NSCLC. Mice were subcutaneously injected with sh-circ_0079530 or sh-NC-transfected H2170 cells, and then the tumors were treated by 4 Gy radiation or not. (**A**) Circ_0079530 level was measured via qRT-PCR in sh-circ_0079530 or sh-NC-transfected H2170 cells (n = 3). (**B**) Tumor volume was measured (n = 6). (**C**) Tumor weight was detected at the end (n = 6). (**D**) PCNA, MMP9, E-cadherin, ICAM-1, and vitronectin levels were examined via western blotting in tumor tissues (n = 6). *P <0.05 **P <0.01 and ***P <0.001. NSCLC: non-small cell lung cancer; qRT-PCR: quantitative reverse transcription-polymerase chain reaction; NC: negative control; PCNA: proliferating cell nuclear antigen; MMP9: matrix metalloproteinase 9; ICAM-1: intercellular adhesion molecule-1
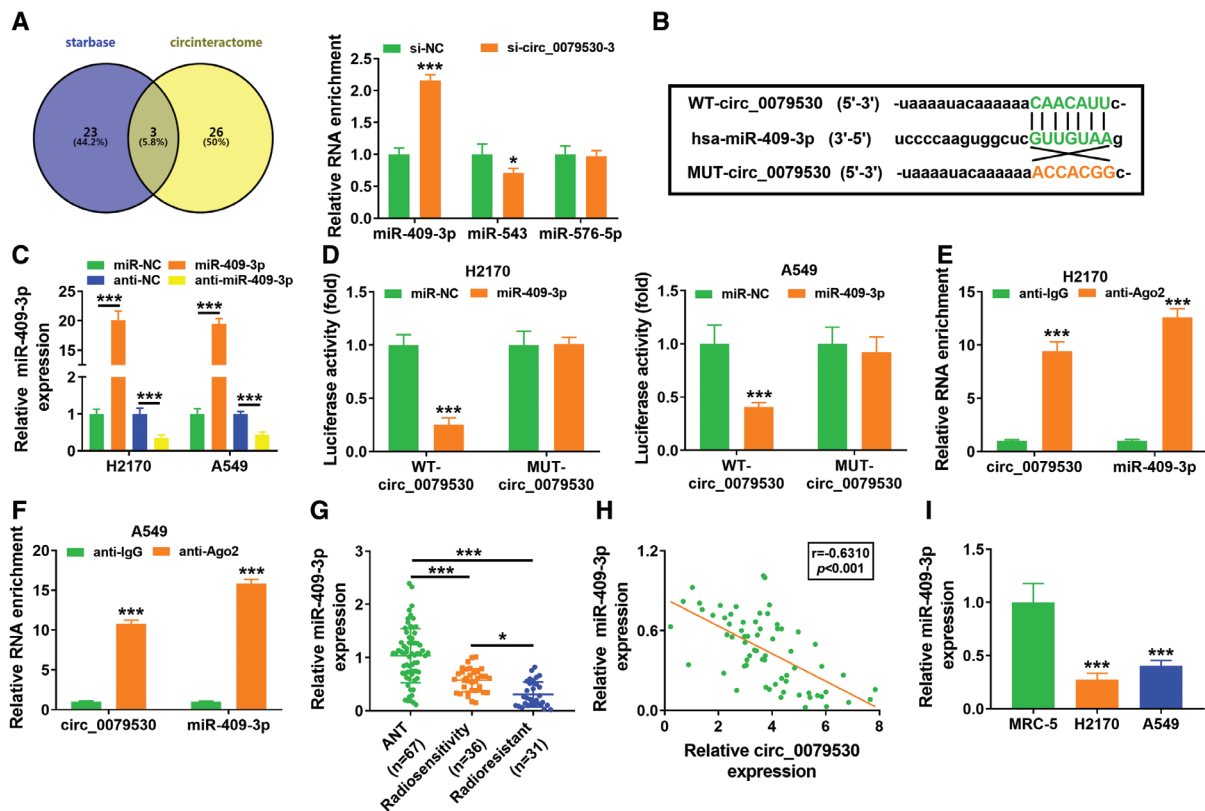
Fig. 3 MiR-409-3p targeted circ_0079530. (**A**) The targets of circ_0079530 were predicted by starBase and circInteractome, and the levels of miR-409-3p, miR-543, and miR-576-5p were measured via qRT-PCR in si-circ_0079530-3 or si-NC-transfected H2170 cells (n = 3). (**B**) The target sites of circ_0079530 and miR-409-3p. (**C**) MiR-409-3p level was determined via qRT-PCR in cells with transfection of miR-NC, miR-409-3p mimic, anti-NC, or anti-miR-409-3p (n = 3). (**D**) Luciferase activity of WT-circ_0079530 and MUT-circ_0079530 was detected via dual-luciferase reporter assay in cells transfected with miR-NC or miR-409-3p mimic (n = 3). (**E and F**) RIP assay was used to analyze the interaction in NSCLC cells (n = 3). (**G**) MiR-409-3p level was measured with qRT-PCR in radiosensitive (n = 36) or radioresistant (n = 31) NSCLC tissues and ANT samples (n = 67). (**H**) The linear correlation between circ_0079530 and miR-409-3p in NSCLC was assessed via the Pearson test (n = 67). (**I**) MiR-409-3p expression was determined via qRT-PCR in MRC5, H2170, and A549 cells (n = 3). *$P <0.05$ and ***$P <0.001$. NSCLC: non-small cell lung cancer; qRT-PCR: quantitative reverse transcription-polymerase chain reaction; NC: negative control; WT: wild type; MUT: mutant; RIP: RNA immunoprecipitation; ANT: adjacent non-tumor tissue

radioresistant (n = 31) tissues compared with that in ANT samples (n = 67), and miR-409-3p expression was lower in radioresistant samples than that in radiosensitive tissues (**Fig. 3G**). Furthermore, the expression of miR-409-3p in NSCLC samples was negatively correlated with circ_0079530 expression (**Fig. 3H**). In addition, miR-409-3p expression was markedly declined in H2170 and A549 cells in comparison to that in MRC-5 cells (**Fig. 3I**). These data showed that circ_0079530 functioned as a miR-409-3p sponge.

MiR-409-3p inhibition mitigates the effects of circ_0079530 interference on cell proliferation, radiosensitivity, migration, and invasion

To explore whether miR-409-3p could affect the function of circ_0079530 in NSCLC, H2170 and A549 cells were transfected with si-NC, si-circ_0079530-3, si-circ_0079530-3 + anti-NC, or si-circ_0079530-3 + anti-miR-409-3p. We observed that miR-409-3p was obviously increased by circ_0079530 silence, but this elevation was reversed by the addition of anti-miR-409-3p (**Supplementary Fig. 2A**). Moreover, miR-409-3p knockdown reversed the suppressive effect of circ_0079530 silence on cell proliferation (**Supplementary Fig. 2B**). In addition, miR-409-3p downregulation attenuated circ_0079530 knockdown-mediated effects on survival fraction after treatment of radiation (**Supplementary Fig. 2C**). Furthermore, miR-409-3p knockdown abolished si-circ_0079530-triggered decline in EdU-positive cells in H2170 and A549 cells treated with 4 Gy radiation (**Supplementary Fig. 2D**). Additionally, miR-409-3p reduction rescued the migratory and
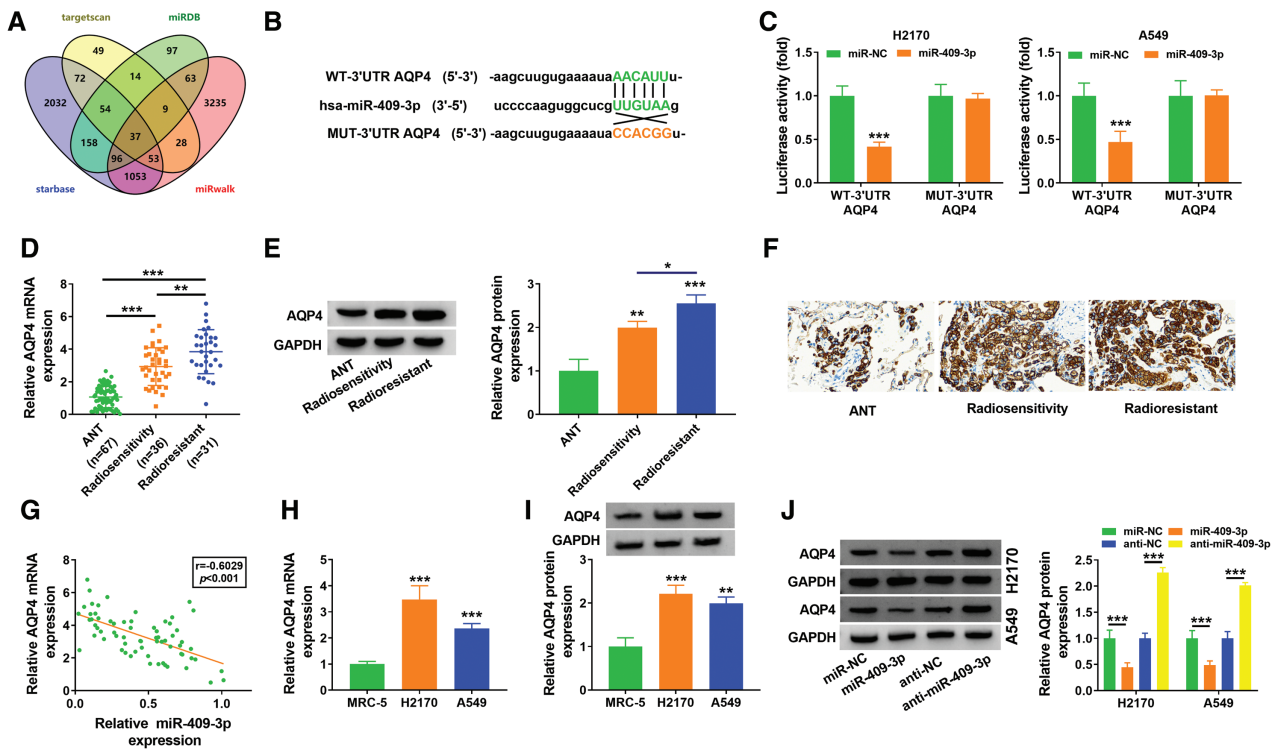
Fig. 4 AQP4 is targeted by miR-409-3p. (**A**) 37 potential target mRNAs of miR-409-3p were predicted by TargetScan, miRDB, starBase, and miRWalk. (**B**) The target sequence of miR-409-3p and AQP4 was searched via starBase. (**C**) Luciferase activity of WT-3'UTR AQP4 and MUT-3'UTR AQP4 was examined using dual-luciferase reporter assay in cells transfected with miR-NC or miR-409-3p mimic (n = 3). (**D and E**) AQP4 abundance was determined by qRT-PCR and western blotting in radiosensitive (n = 36) or radioresistant (n = 31) NSCLC tissues and ANT samples (n = 67). (**F**) Immunohistochemical staining was applied to detect AQP4 expression in normal tissues and NSCLC tissues. (**G**) The linear correlation between miR-409-3p and AQP4 in NSCLC tissues was analyzed via the Pearson test (n = 67). (**H and I**) AQP4 expression was determined via qRT-PCR and western blotting in MRC5, H2170, and A549 cells (n = 3). (**J**) AQP4 level was examined via western blotting in cells transfected with miR-NC, miR-409-3p mimic, anti-NC, or anti-miR-409-3p (n = 3). *$P <0.05$, **$P <0.01$, and ***$P <0.001$. AQP4: aquaporin 4; NSCLC: non-small cell lung cancer; qRT-PCR: quantitative reverse transcription-polymerase chain reaction; NC: negative control; WT: wild type; UTR: untranslated region; MUT: mutant; ANT: adjacent non-tumor tissue

invasive abilities under radiation conditions (**Supplementary Figs. 2E** and **2F**). Besides, miR-409-3p knockdown reversed the upregulation of E-cadherin and the downregulation of ICAM-1 and vitronectin in radiation-challenged H2170 and A549 cells caused by circ_0079530 silencing (**Supplementary Figs. 2G** and **2H**). These results suggested that circ_0079530 regulated NSCLC progression and radiosensitivity by modulating miR-409-3p expression.

AQP4 is targeted via miR-409-3p

Next, 37 potential targets of miR-409-3p were predicted by TargetScan, miRDB, starBase, and miRWalk (**Fig. 4A**). Of all these mRNAs, we selected 8 mRNAs (LRP6, UBE2N, CCND2, KLF12, AQP4, ONECUT2, GAB1, and LARP1) related to NSCLC progression for further analysis. As exhibited in **Supplementary Fig. 3**,

the mRNA level of AQP4 was overtly repressed in miR-409-3p-overexpressed H2170 cells compared to that of other mRNAs. Thus, AQP4 was selected as a candidate target, and the binding sites of miR-409-3p and AQP4 are displayed in **Fig. 4B**. In order to validate this prediction, the WT-3'UTR AQP4 and MUT-3'UTR AQP4 luciferase reporter vectors were constructed. As shown in **Fig. 4C**, miR-409-3p overexpression clearly decreased the luciferase activity of WT-3'UTR AQP4, while it did not alter the activity of MUT-3'UTR AQP4. Furthermore, the mRNA and protein levels of AQP4 were obviously enhanced in radiosensitive (n = 36) and radioresistant (n = 31) tissues compared with those in ANT samples (n = 67), and AQP4 mRNA and protein levels were increased in radioresistant samples compared with those in radiosensitive tissues (**Figs. 4D** and **4E**). Besides, IHC staining showed that the expression

of AQP4 was increased in NSCLC tissues relative to that in normal tissues (**Fig. 4F**). Meanwhile, AQP4 mRNA expression in NSCLC tissues was negatively associated with miR-409-3p expression (**Fig. 4G**). In addition, the mRNA and protein levels of AQP4 were markedly upregulated in H2170 and A549 cells in comparison to those in MRC-5 cells (**Figs. 4H** and **4I**). Moreover, the protein levels of AQP4 were decreased by miR-409-3p overexpression and increased by miR-409-3p knockdown in H2170 and A549 cells (**Fig. 4J**). These findings indicated that AQP4 was targeted by miR-409-3p in NSCLC.

MiR-409-3p restrains cell proliferation, migration, and invasion, and facilitates radiosensitivity by modulating AQP4 expression

We then verified the overexpression efficiency of the AQP4 overexpression plasmid, and the results exhibited that the levels of AQP4 protein were enhanced after transfection of AQP4 overexpression plasmid (**Fig. 5A**). To study the role of miR-409-3p/AQP4 axis in NSCLC, H2170 and A549 cells were transfected with miR-NC, miR-409-3p mimic, miR-409-3p mimic + AQP4 overexpression, or miR-409-3p mimic + pcDNA. The addition of AQP4 overexpression vector effectively impaired the elevation of AQP4 mediated by miR-409-3p mimic (**Fig. 5B**). CCK-8 assay showed that miR-409-3p overexpression markedly decreased the proliferation of H2170 and A549 cells, and this effect was rescued by the addition of AQP4 overexpression vector (**Fig. 5C**). Moreover, miR-409-3p overexpression obviously inhibited the survival fraction after radiation treatment, and this effect was abolished by AQP4 upregulation (**Fig. 5D**). Additionally, miR-409-3p upregulation clearly reduced the number of EdU positive cells in radiation-challenged H2170 and A549 cells, while the introduction of pcDNA–AQP4 could overturn this effect (**Fig. 5E**). Furthermore, miR-409-3p mimic evidently decreased cell migration and invasion in radiation-challenged cells, which these impacts were relieved via AQP4 upregulation (**Figs. 5F** and **5G**). Additionally, miR-409-3p overexpression resulted in a significant increase in E-cadherin protein levels and a marked reduction in ICAM-1 and vitronectin protein levels in cells with radiation treatment, while these events were abolished by AQP4 introduction (**Figs. 5H** and **5I**). These results showed that miR-409-3p suppressed NSCLC progression and increased radiosensitivity by targeting AQP4.

Circ_0079530 modulates AQP4 expression through miR-409-3p

To analyze if circ_0079530 could regulate AQP4 in NSCLC, AQP4 protein levels in H2170 and A549 cells transfected with si-NC, si-circ_0079530-3, si-circ_0079530-3 + anti-NC, or si-circ_0079530-3 + anti-miR-409-3p under 4 Gy radiation treatment were detected. As exhibited in **Supplementary Fig. 4A**, AQP4 protein levels were markedly downregulated by circ_0079530 interference, but this downregulation was restored by miR-409-3p knockdown. The schematic diagram of this research is shown in **Supplementary Fig. 4B**, which showed that circ_0079530 enhanced AQP4 expression by functioning as a miR-409-3p sponging, thus affecting NSCLC progression and radiosensitivity.

Discussion

NSCLC is the main subtype of lung cancer with high incidence and mortality.[2] CircRNAs can function as important regulators in NSCLC progression and have potential value in NSCLC therapy.[21] This research mainly explored how circ_0079530 took part in NSCLC development and radiosensitivity. We found circ_0079530 silence inhibited NSCLC progression and increased radiosensitivity by the miR-409-3p/AQP4 axis.

A former study suggested that circ_0079530 facilitated NSCLC proliferation and invasion.[11] Similarly, we also found the repressive effects of circ_0079530 silence on NSCLC cell proliferation and metastasis. Furthermore, our study found that circ_0079530 expression was changed in radiosensitive and radioresistant patients, suggesting that increased circ_0079530 expression might be associated with radiosensitivity in NSCLC. Through exposure to different doses of radiation, we found that circ_0079530 knockdown enhanced NSCLC cell radiosensitivity. The cell cycle, migration, and invasion are important processes associated with resistant progression.[22,23] Adhesion molecules (E-cadherin, ICAM-1, and vitronectin) play important roles in cell migration and invasion.[24–26] By transwell assay and detecting these molecules, we found that circ_0079530 interference decreased cell migration and invasion via increasing E-cadherin and decreasing ICAM-1 and vitronectin in cells under radiation. Furthermore, by detecting tumor growth and related proteins (PCNA, MMP9, E-cadherin, ICAM-1, and vitronectin) in tumor tissues, we found that circ_0079530 knockdown decreased
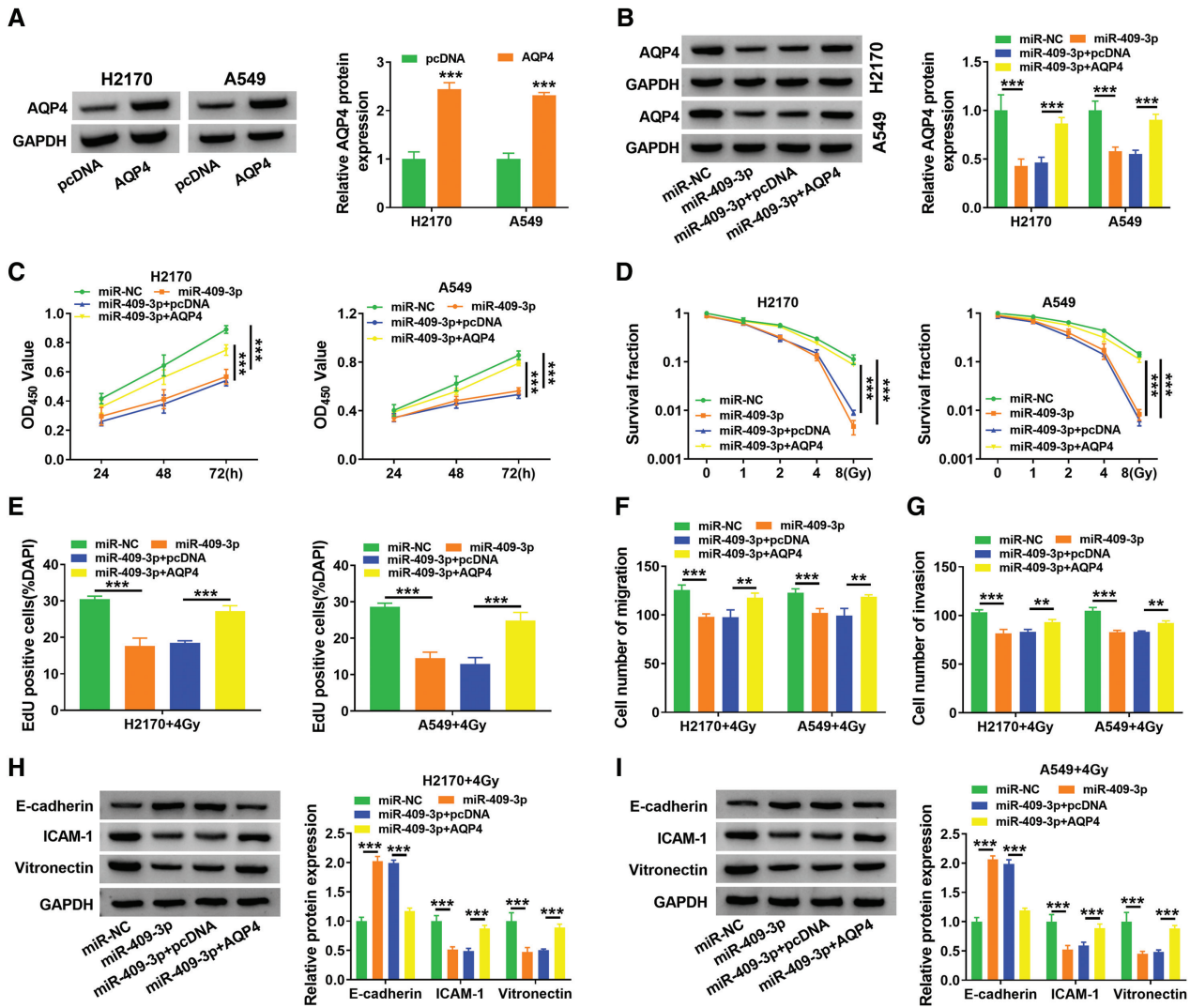
Fig. 5 MiR-409-3p decreases cell proliferation, migration, and invasion, and enhances radiosensitivity by modulating AQP4 in NSCLC. (**A**) AQP4 level was detected via western blotting in cells transfected with AQP4 overexpression vector or pcDNA (n = 3). H2170 and A549 cells were transfected with miR-NC, miR-409-3p mimic, miR-409-3p mimic + AQP4 overexpression vector, or pcDNA. (**B**) AQP4 expression was measured via western blotting in the transfected cells (n = 3). (**C**) Cell proliferation was measured with CCK-8 in the transfected cells (n = 3). (**D**) The radiosensitivity was analyzed by survival fraction using colony formation assay in the transfected cells after treatment of various doses of radiation (n = 3). (**E**) 5-ethynyl-2'-deoxyuridine (EdU)-positive cells were measured via EdU assay in the transfected cells after exposure to 4 Gy radiation (n = 3). (**F** and **G**) Cell migration and invasion were examined using transwell assay in the transfected cells after treatment with 4 Gy radiation (n = 3). (**H** and **I**) E-cadherin, ICAM-1, and vitronectin abundances were detected via western blotting in the transfected cells after treatment with 4 Gy radiation (n = 3). **P <0.01 and ***P <0.001. AQP4: aquaporin 4; NSCLC: non-small cell lung cancer; NC: negative control; CCK-8: cell counting kit-8; ICAM-1: intercellular adhesion molecule-1

tumor growth under radiation in xenograft models. Collectively, targeting circ_0079530 might be used to treat NSCLC and enhance radiosensitivity.

Next, we explored a circRNA–miRNA–mRNA network mediated by circ_0079530, which was the main mechanism underlying the role of circRNA in NSCLC.[27] By analyzing the targets of circ_0079530, we confirmed that miR-409-3p targeted circ_0079530. Multiple pieces of

evidence suggested miR-409-3p repressed cell proliferation, migration, and invasion in NSCLC.[16] Similarly, our study also identified the antitumor activity of miR-409-3p. Moreover, we first found that miR-409-3p might act as a sensitizing agent for radiation in NSCLC by increasing radiosensitivity. Additionally, our study showed that circ_0079530 could mediate NSCLC progression and radiosensitivity by miR-409-3p. Furthermore, we confirmed

AQP4 as a downstream target of miR-409-3p. AQP4, a member of the AQP family, is distributed in the membrane of various biological cells.[28] AQP4 is responsible for maintaining nerve excitation, cell migration, and water homeostasis in the brain.[29] It has been reported that AQP4 is highly expressed in lung adenocarcinoma tissues, and AQP4 contributes to NSCLC cell invasion.[18] AQP4 was associated with radiotherapy in breast cancer.[30] Here, we validated miR-409-3p could restrain NSCLC progression and radiosensitivity via targeting AQP4. In addition, we confirmed that circ_0079530 could mediate AQP4 by sponging miR-409-3p. The current work concluded that the circ_0079530/miR-409-3p/AQP4 axis modulated NSCLC progression and radiosensitivity.

Conclusion

In conclusion, circ_0079530 interference constrained NSCLC progression and increased radiosensitivity via the miR-409-3p/AQP4 axis, at least in part. This study provided a new insight into NSCLC development and radiosensitivity and supported circ_0079530 as a target for the treatment of NSCLC.

Ethics Approval and Consent to Participate

The present study was approved by the ethical review committee of Changsha Central Hospital. Written informed consent was obtained from all enrolled patients. Patients agreed to participate in this work.

Data Availability Statement

The analyzed data sets generated during the present study are available from the corresponding author on reasonable request.

Authors' Contribution

All authors made substantial contribution to conception and design, acquisition of the data, or analysis and interpretation of the data; took part in drafting the article or revising it critically for important intellectual content; gave final approval of the revision to be published; and agreed to be accountable for all aspects of the work.

Disclosure Statement

The authors declare that they have no competing interests.

References

1) Hirsch FR, Scagliotti GV, Mulshine JL, et al. Lung cancer: current therapies and new targeted treatments. Lancet 2017; **389**: 299–311.
2) Schabath MB, Cote ML. Cancer progress and priorities: lung cancer. Cancer Epidemiol Biomarkers Prev 2019; **28**: 1563–79.
3) Duma N, Santana-Davila R, Molina JR. Non-small cell lung cancer: epidemiology, screening, diagnosis, and treatment. Mayo Clin Proc 2019; **94**: 1623–40.
4) Yang WC, Hsu FM, Yang PC. Precision radiotherapy for non-small cell lung cancer. J Biomed Sci 2020; **27**: 82.
5) Jakobi T, Dieterich C. Computational approaches for circular RNA analysis. Wiley Interdiscip Rev RNA 2019; **10**, e1528.
6) Li C, Zhang L, Meng G, et al. Circular rnas: pivotal molecular regulators and novel diagnostic and prognostic biomarkers in non-small cell lung cancer. J Cancer Res Clin Oncol 2019; **145**: 2875–89.
7) Wei S, Zheng Y, Jiang Y, et al. The circRNA circPT-PRA suppresses epithelial-mesenchymal transitioning and metastasis of nsclc cells by sponging mir-96-5p. EBioMedicine 2019; **44**: 182–93.
8) Hong W, Xue M, Jiang J, et al. Circular RNA circ-CPA4/ let-7 miRNA/PD-L1 axis regulates cell growth, stemness, drug resistance and immune evasion in non-small cell lung cancer (NSCLC). J Exp Clin Cancer Res 2020 **39**: 149.
9) Liang ZZ, Guo C, Zou MM, et al. CircRNA-miR-Na-mRNA regulatory network in human lung cancer: an update. Cancer Cell Int 2020; **20**: 173.
10) Li YH, Xu CL, He CJ, et al. Circmtdh.4/mir-630/aeg-1 axis participates in the regulation of proliferation, migration, invasion, chemoresistance, and radioresistance of nsclc. Mol Carcinog 2020; **59**: 141–53.
11) Li J, Wang J, Chen Z, et al. Hsa_circ_0079530 promotes cell proliferation and invasion in non-small cell lung cancer. Gene 2018; **665**: 1–5.
12) Petrek H, Yu AM. Micrornas in non-small cell lung cancer: Gene regulation, impact on cancer cellular processes, and therapeutic potential. Pharmacol Res Perspect 2019; e00528.
13) Liu ZL, Wang H, Liu J, et al. MicroRNA-21 (miR-21) expression promotes growth, metastasis, and chemo- or radioresistance in non-small cell lung cancer cells by targeting PTEN. Mol Cell Biochem 2013; **372**: 35–45.
14) Yang YB, Tan H, Wang Q. MiRNA-300 suppresses proliferation, migration and invasion of non-small cell lung cancer via targeting ETS1. Eur Rev Med Pharmacol Sci 2019; **23**: 10827–34.
15) Yin D, Hua L, Wang J, et al. Long non-coding RNA DUXAP8 facilitates cell viability, migration, and glycolysis in non-small-cell lung cancer via regulating HK2 and LDHA by inhibition of miR-409-3p. Onco Targets Ther 2020; **13**: 7111–23.
16) Liu S, Li B, Xu J, et al. SOD1 promotes cell proliferation and metastasis in non-small cell lung cancer via

an miR-409-3p/SOD1/SETDB1 epigenetic regulatory feedforward loop. Front Cell Dev Biol 2020; **8**: 213.

17) Song Y, Wang L, Wang J, et al. Aquaporins in respiratory system. Adv Exp Med Biol 2017; **969**: 115–22.

18) Xie Y, Wen X, Jiang Z, et al. Aquaporin 1 and aquaporin 4 are involved in invasion of lung cancer cells. Clin Lab 2012; **58**: 75–80.

19) Levy M, Barletta S, Huang H, et al. Aquaporin-4 expression patterns in glioblastoma pre-chemoradiation and at time of suspected progression. Cancer Invest 2019; **37**: 67–72.

20) Sohaib A. Recist rules. Cancer Imaging 2012; **12**: 345–6.

21) Zhang C, Ma L, Niu Y, et al. Circular RNA in lung cancer research: Biogenesis, functions, and roles. Int J Biol Sci 2020; **16**: 803–14.

22) Alimbetov D, Askarova S, Umbayev B, et al. Pharmacological targeting of cell cycle, apoptotic and cell adhesion signaling pathways implicated in chemoresistance of cancer cells. Int J Mol Sci 2018; **19**: 1690.

23) Assani G, Zhou Y. Effect of modulation of epithelial-mesenchymal transition regulators snail1 and snail2 on cancer cell radiosensitivity by targeting of the cell cycle, cell apoptosis and cell migration/invasion. Oncol Lett 2019; **17**: 23–30.

24) Canel M, Serrels A, Frame MC, et al. E-cadherin-integrin crosstalk in cancer invasion and metastasis. J Cell Sci 2013; **126**: 393–401.

25) Bui TM, Wiesolek HL, Sumagin R. ICAM-1: A master regulator of cellular responses in inflammation, injury resolution, and tumorigenesis. J Leukoc Biol 2020; **108**: 787–99.

26) Singh B, Su YC, Riesbeck K. Vitronectin in bacterial pathogenesis: a host protein used in complement escape and cellular invasion. Mol Microbiol 2010; **78**: 545–60.

27) Cai X, Lin L, Zhang Q, et al. Bioinformatics analysis of the circRNA-miRNA-mRNA network for non-small cell lung cancer. J Int Med Res 2020; **48**: 300060520929167.

28) Agre P, Sasaki S, Chrispeels MJ. Aquaporins: a family of water channel proteins. Am J Physiol 1993; **265**: F461.

29) Papadopoulos MC, Verkman AS. Aquaporin water channels in the nervous system. Nat Rev Neurosci 2013; **14**: 265–77.

30) Stumpf PK, Cittelly DM, Robin TP, et al. Combination of trastuzumab emtansine and stereotactic radiosurgery results in high rates of clinically significant radionecrosis and dysregulation of aquaporin-4. Clin Cancer Res 2019; **25**: 3946–53.